Article
https://doi.org/10.31489/2024PH4/46-53
UDC 536-12; 544.454.2
Received: 21.06.2024
Accepted: 19.08.2024

A.V. Kalenskii*, A.A. Zvekov, A.P. Borovikova, E.V. Galkina, P.O. Vinodiktov

Kemerovo State University, Kemerovo, Russia
*(*Corresponding author's e-mail: kalenskyav@gmail.com)*

The laser initiation of energetic materials doped with metal nanoparticles having oxide shell explosive decomposition

The work is devoted to the development of the model describing laser initiation composite materials being an explosive matrix with metal nanoparticles covered with oxide shell. The model considers the oxide shell as a dielectric that does not absorb light. The example of aluminum nanoparticles covered with alumina is the main one in the paper. The model describes the thermal transfer in the system metal core-oxide shell-explosive material, exothermic decomposition of the explosive considered as a one-step reaction with Arrhenius dependence on the rate on temperature, and light absorption of the core-shell interface. The model is written as a system of the equations and respective computer program is developed. The semi-quantitative analysis of the model using the typical thickness of the heated layer of the matrix is performed. It is shown that the radius of the nanoparticle heated most is proportional to the thickness of the heated layer of the explosive matrix as in the previous versions of the model though the coefficient depends on the oxide shell thickness. The numerical analysis is done. The dependencies of critical energy density on the oxide shell thickness at constant nanoparticle's radius and on the radius at constant shell thickness are calculated. The dependence on radius shows the existence of the optimal particle minimizing the critical energy density whose radius depends on the shell thickness.

Keywords: laser initiation, thermal explosion, hot-spot model, core-shell nanoparticles, energetic materials.

Introduction

The development of laser initiation approaches of explosive decomposition is essential for safety increasing in the explosives' utilization as well as for ecology risks and technological catastrophes minimization. One of the solution steps of this relevant task is the development of explosive blends selectively sensible to laser impact. The decreasing of neodymium laser pulse critical energy density of pentaerythritol tetranitrate (PETN) explosion in one hundred times was achieved earlier by mixing the explosive with aluminum nanoparticles [1]. The significant influence (13 times) of the oxide shell of the nanoparticles on the critical energy density of the PETN initiation was discovered in [2]. The respective model was suggested in [3].

The optic detonators based on primary explosives such as silver azide have not been applied extensively as they show low thresholds not only to laser impact but also to heat and electric stimulus. Another ways of the problem solution are development of optic detonators based on the high-energy metal complexes with nitrogen-rich ligands [4, 5] or application of secondary explosives which critical energy density of the laser impact was diminished with some additives. The sensibilization of the transparent secondary explosives was done with metal nanoparticles introduced in small quantities (about 1 %) in the works [1, 6, 7]. Significant decreasing in the critical energy density of the laser pulse appears due to both effective linear absorption coefficient increasing [8] and heating of just nanoparticles and thin layer of the explosive around it that is a negligible part of the sample. For that reason, the minimal energy density of secondary explosive PETN laser initiation with aluminum [6, 7], nickel and cobalt [9, 10] is about 1 J/cm^2 at the main wavelength of the neodymium laser. The perspectives of gold nanoparticles with diameter 60 nm showing maximum of the plasmon resonance band at 532 nm as a sensibilizing additive to hexogen comparing to carbon particles of soot and nanotubes was pointed out in [11]. Several papers were devoted to changing of the nanoparticles' shape aiming at fitting the plasmon absorption band to the wavelength of the commercially available continuous-wave lasers [12–15]. The sensibilization of 1,1-diamino-2,2-dinitroethene with gold nanorods was performed in [12] that made it possible to initiate them with continuous-wave laser at 808 nm and power 8 W with reaching the pressure of 1.5 GPa at the rear side of the charge which is enough for the typically secondary explosives' detonation initiation. The additive of black carbon leads to initiation threshold of 17 W in similar conditions [13]. The application of gold-copper alloy additives in the nano-stars shape allows one to initiate

hexogen with continuous-wave laser irradiation at power 41 W which is 6 times lower than for pure hexogen [14]. Silver nano-plates of various shapes (round, triangle, and cracked triangles) utilization showed that the cracked triangles are the most efficient as hexogen sensibilizing additives though the absorption spectra of the samples are close [15].

The micro hot-spot conception of the thermal explosion based on the light absorption by metal nanoparticles in the explosive's volume was suggested in [16] for silver and lead azides. The relevance of the optic detonators using secondary explosives linked with safety issues attracted researchers to this model. The hot-spot model applied to secondary explosives initiation was formulated in [1, 8, 10, 17] with phase transitions and optical properties of the composites taking into account. As a result, the most of experimental data on the laser pulse initiation of explosives found qualitative and partly quantitative explanation, including the dependence of the critical energy density on the pulse duration. A few new effects were predicted and discovered afterwards such as dependence of the initiation threshold on the laser wavelength, radius and mass fraction of the sensibilizing nanoparticles. The dielectric shell of the nanoparticles was included in the hot-spot model in [3] where its influence on the optic and thermal properties was discussed. The calculation of absorption and scattering efficiency factors of the nanoparticles with metal core-dielectric shell structure was performed. The maximum temperatures of the core-shell particles heated in the inert medium were calculated varying the nanoparticle's radius. It was shown that oxide shell changes drastically the optic properties of the nanoparticle. The further research into hot-spot model is relevant due to their fundamental significance in the point of mechanisms of laser initiation understanding and practice linked with optic detonators' composition optimization.

The aim of the present work is research into laser initiation regularities of PETN taking into account oxide shell of the aluminum sensibilizing nanoparticle. The main task is to perform the kinetic analysis of the composites PETN/Al/Al_2O_3 laser initiation model at variation of the both nanoparticle's radius and shell thickness in the wide range. The model is analyzed for the practically important case of composite PETN-aluminum nanoparticles. The dependence of the critical energy density on this composite on the oxide content in the nanoparticle was studied experimentally earlier [2].

The hot-spot model of laser initiation in the case of core-shell nanoparticles

The differential equations of the hot-spot model in the core-shell particle case are as follows [3]:

$$\begin{aligned}
&\frac{\partial T}{\partial t} = \alpha \cdot \left(\frac{\partial^2 T}{\partial x^2} + \frac{2}{x} \cdot \frac{\partial T}{\partial x} \right) + k_0 \frac{nQ}{c} \cdot \exp\left(-\frac{E}{k_B T} \right) && x>R \\
&\frac{\partial n}{\partial t} = -k_0 n \cdot \exp\left(-\frac{E}{k_B T} \right) && x>R \\
&\frac{\partial T}{\partial t} = \alpha_0 \left(\frac{\partial^2 T}{\partial x^2} + \frac{2}{x} \cdot \frac{\partial T}{\partial x} \right) && r<x<R \\
&\frac{\partial T}{\partial t} = \alpha_M \left(\frac{\partial^2 T}{\partial x^2} + \frac{2}{x} \cdot \frac{\partial T}{\partial x} \right) && x<r \\
&\frac{\partial n}{\partial t} = 0 \text{ , } n=0, && x<R
\end{aligned} \qquad (1)$$

where lower index 0 marks the shell, *M* marks the core, α is thermal diffusivity, *c* is volumic heat capacity, *n* is the content of the unreacted explosive substance, k_0 is preexponential factor, *E* is activation energy, *Q* is heat released at decomposition of 1 cm^3 of the explosive substance, *R* is nanopartciles radius, *r* is radius of the core. The metal core absorbs light in the core of core-shell particles case. The energy absorbed is consumed on heating the core then the shell is heated and only after it the heat is transferred to the surrounding explosive's layer initiating its decomposition.

Thus, on the boundaries shell-explosive and core-shell respective boundary conditions arise making contrast to initial micro hot-spot model:

$$-c_0\alpha_0 \cdot \frac{\partial T}{\partial x}\Big|_{(x\to R-0)} + c\alpha \cdot \frac{\partial T}{\partial x}\Big|_{(x\to R+0)} = 0 \tag{2.a}$$

$$J - c_M\alpha_M \cdot \frac{\partial T}{\partial x}\Big|_{x\to r-0} + c_0\alpha_0 \cdot \frac{\partial T}{\partial x}\Big|_{x\to r+0}. \tag{2.b}$$

The calculations were done using parameters from [1–3]. The temporal dependence of the function J was taken in the normal distribution shape according to the pulse shape of the experimentally used lasers [10]. It is reasonable to get rid of one of the parameters counting time from the pulse maximum and starting calculation earlier (3):

$$J(t) = \sqrt{\pi} \cdot Q_{abs} R^2 k_i H_0 \cdot \exp\left(-k_i^2 t^2\right), \tag{3}$$

where k_i determines the pulse duration at the half width according to the expression $\tau = 2 \cdot k_i / \sqrt{\ln 2}$. The value of absorption efficiency Q_{abs} determines the intensity of light interaction with nanoparticle and we discussed it thoroughly in [18, 19].

Results and discussion

An important task in the model analysis is determination of the nanoparticle's radius heated by the laser pulse to maximum temperature neglecting the explosive's decomposition. Denoting $\sqrt{\frac{3c}{c_1}}$ as K in the case of micro hot-spot model this radius is proportional to the matrix heated layer thickness $R_m = Kh$, where $h \approx \sqrt{2\alpha / k_i}$, while the maximum temperature augmentation takes form:

$$\delta T = \frac{\pi RH}{4/3\,\pi c_1 R^2 + 4\pi c\left(Rh + h^2\right)} = = \frac{\pi KhH}{4/3\,\pi \frac{3c}{K^2} h^2 K^2 + 4\pi c\left(hKh + h^2\right)} = \frac{KH}{4ch(K+2)}. \tag{4}$$

A similar analysis was performed in the case of the core-shell particles. The estimation of the maximum heating temperature in the case of particle having oxide shell with thickness (R — r) we will use the ration of nanoparticles and core radii $Z = R/r$. The expression for temperature augmentation can be written as follows:

$$\Delta T = \frac{Q}{c} = \frac{H \cdot \pi r^2}{c_A \cdot \frac{4}{3}\pi r^3 + c_0 \cdot \frac{4}{3}\pi r^3\left(Z^3 - 1\right) + c_m 4\pi Z^2 r^2 h + 4\pi c_m h^2 Z r}.$$

The particles with the most pronounced temperature increasing are determined applying maximum conditions:

$$\Delta T' = 0$$

$$\left(\frac{H \cdot r^2}{r^3\left(\frac{4}{3}c_A + \frac{4}{3}c_0 \cdot \left(Z^3 - 1\right)\right) + 4c_m Z^2 r^2 h + 4c_m h^2 Z r}\right)' = 0 \tag{5}$$

$$R_m = \sqrt{\frac{3c_m Z h^2}{c_A - c_0 \cdot \left(Z^3 - 1\right)}}.$$

It can be deduced from (5) that the radius of the most heated nanoparticle R_m does not depend on the pulse energy density but depends on pulse duration which presents through the thickness of the matrix heated layer h. For that reason, we calculated the dependence of the maximum temperature of the heated nanoparticle in the inert matrix with PETN parameters on the radius at different pulse durations. The results are shown in Figures 1 and 2 at the pulse duration 14 and 20 ns respectively. The energy density values were 25, 50, and 75 mJ/cm^2. The ration of core and nanoparticle radii was 0.75. The range of radii was taken rather wide, so the value of R_m fell in it. The self-accelerating mode of the reaction was excluded due to taking preexponential factor equal to 0.

At the energy density value 25 mJ/cm^2 the maximum temperature increases from 437 to 604 K when radius increases from 10 to 60 nm and is decreased to 565 K as the radius gets to 120 nm. When the energy density increases to 50 J/cm^2, the maximum temperature of the nanopartilces increases to 538 K for 10 nm and 909 K for 60 nm, while it becomes equal to 835, if the radius is 120 nm. If the energy density is 75 J/cm^2 the respective maximum temperatures for 10, 60 and 120 nm particle radii are 710, 1213 and 1102 K. The augmentation of temperature is proportional to the energy density of the pulse. The most heated particle has radius 60 nm in this case.

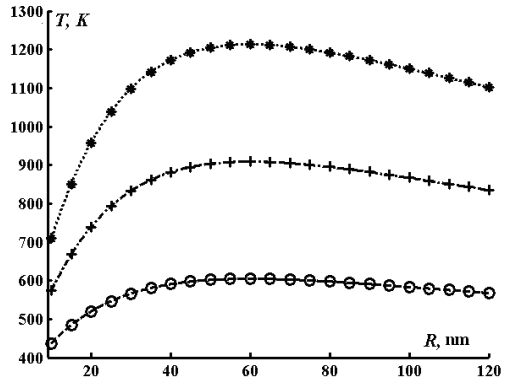

Figure 1. Calculated dependencies of the maximum temperature of the aluminum nanoparticles heated in PETN on its radius at r/R=0.75 and pulse duration 14 ns.

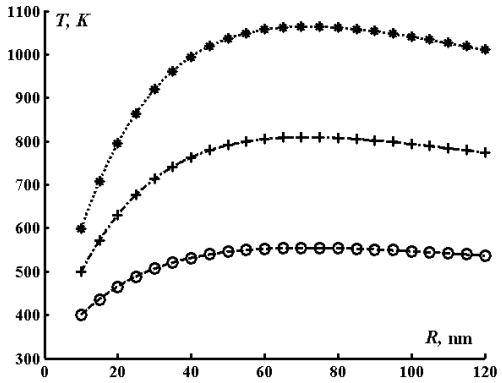

Figure 2. Calculated dependencies of the maximum temperature of the aluminum nanoparticles heated in PETN on its radius at r/R=0.75 and pulse duration 20 ns.

Figure 2 shows similar dependencies of maximum temperature of the aluminum nanoparticle at the pulse duration 20 ns. Other conditions are the same. The maximum temperature of the particle heated with 20 ns pulse and energy density 25 J/cm^2 is 555 K when radius is 71.8 nm. The temperature decreases for both smaller and bigger particles reaching 399 K at 10 nm and 536 at 120 nm. The maximum temperatures for energy density 75 J/cm^2 for 10, 71.8, and 120 nm are 600, 1064, and 1010 K. Thus the maximum heating temperature is achieved at the definite radius of the nanoparticle dependent on the pulse duration and independent on its energy or power density.

We analyzed thoroughly the temperature distributions in the heating of aluminum nanoparticles covered with alumina in the PETN matrix at the minimal pulse energy density provided explosive decomposition. The temperature distribution arising at the energy density 137 mJ/cm^2 in the case of nanoparticle's radius 50 nm with core radius 35 nm and shell thickness 15 nm are presented in Figure 3. The moments of time counted from the pulse maximum are shown on the legend; they correspond to the slow temperature evolution in the reaction hot-spot linked with reaction energy releasing and heat transfer competition [20].

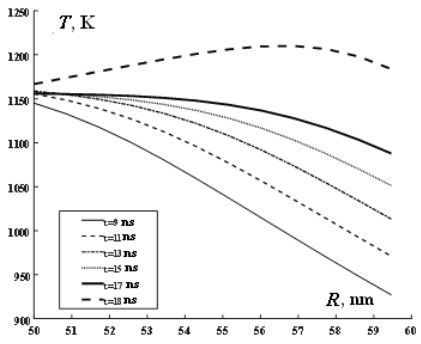

Figure 3. Temperature distributions in PETN at the time moments shown on the legend in the PETN layer surrounding the nanoparticle with radius 50 nm (35 nm core and 15 shell thickness)

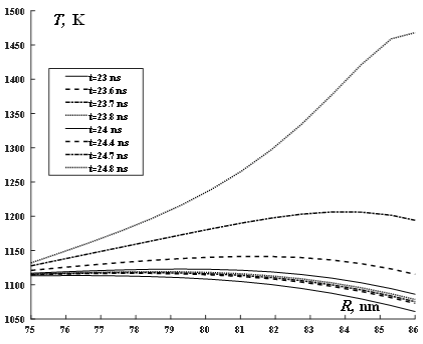

Figure 4. Temperature distributions in PETN surrounding nanoparticle with radius 75 nm (50 nm core and 25 nm shell) at the time momonts shown in the legend

The maximum temperature 1145.1 K is observed on the boundary oxide shell- PETN (50 nm) and the hot-spot thickness is estimated as 2.6 nm at the time 9 ns when the pulse intensity is only 0.318 % of the maximal one. We determined here the hot-area as the part of the PETN matrix where the second derivative is negative as it has to be positive inside the matrix in the case of exothermic reaction absence. Further at time 17 ns the temperature maximum increases to 1155.8 K while the hot layer is widened to 8.8 nm. The pulse intensity at 17 ns is 0.0168 % of the maximum one. Then at 18 ns the temperature on the alumina shell — PETN boundary increases to 1170 K; the hot layer thickness increases to 12.5 nm. It is essential that heat evolving in the exothermal reaction forms temperature maximum leading to explosive decomposition.

Figure 4 shows the temperature distributions in PETN matrix in the case of nanoparticle with radius 75 nm (50 nm core radius and 15 nm shell thickness) in the case of energy density 104.17 mJ/cm^2. The temperature on the boundary decreases slightly between 23 and 24 ns. At the same time the layer of the heated PETN widens, so the temperature gradient decreases. For that reason at time moment 24 ns the heating from the exothermal decomposition reaction overcomes the heat transferring from the hot layer and the temperature increasing begins. The temperature jumps rapidly at the time moment 24.8 ns counting from the pulse maximum evidencing the beginning of the explosive decomposition at the given energy density of the pulse.

Thus, the analysis of temperature field evolution in the system PETN — aluminum nanoparticle with alumina shell varying the energy density of the laser pulse gives one an opportunity to estimate the critical energy density.

The method of the explosive decomposition critical parameters calculation in the case of the composites PETN — aluminum nanoparticles covered with alumina is close to used earlier [20]. In the case of interest one needs to take into account the thermal transfer in the oxide shell. The developed computer program calculated critical energy density H_c at given nanoparticle's radius, radius of the core, shell thickness, and pulse duration. The results are presented in Figure 5 as dependencies of critical energy density of the PETN explosive decomposition on the nanoparticlers' shell thickness at the definite radii of the nanoparticles in the radius range from 15 to 70 nm and shell thickness range from 0 to 30 nm. The calculations were done in the assumption of the absorption cross section equality to the geometrical one.

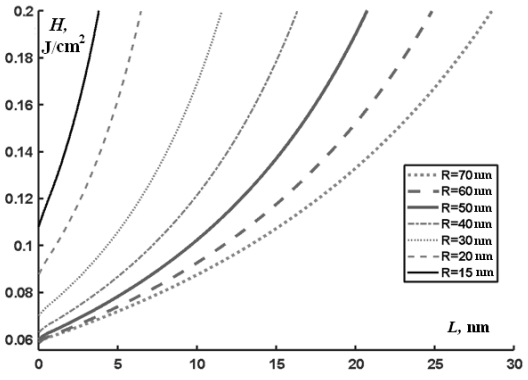

Figure 5. The calculated dependencies of laser pulse critical energy density of PETN- Al/Al_2O_3 explosive decomposition on the oxide shell thickness at definite nanoparticles' radii presented on the legend

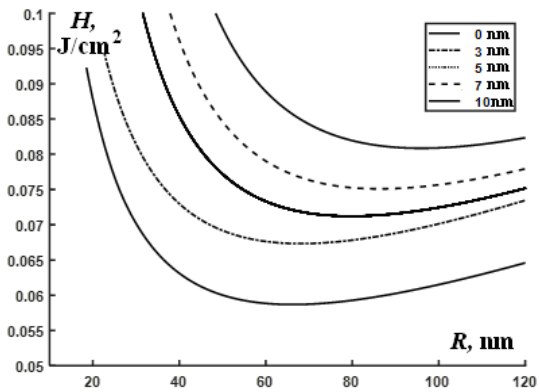

Figure 6. The calculated dependencies $H_c(R)$ for unoxidized aluminum nanoparticles and with oxide shell thickness shown on the legend

The dependencies (Fig. 5) show the increasing of critical energy density when the thickness of the oxide shell increases. It means that the function extremum lays at the zero thickness of the oxide shell minimizing the critical energy density. On the other hand, if one presents the calculation results as dependencies of critical energy density on the nanoparticles' radius at definite oxide shell thickness the minimum points appear (Fig. 6). Thus, as for original hot-spot model of laser initiation in the model taking into account the oxide shell discussed the radius of the most heated nanoparticle (or the optimal radius) appears, but it becomes a function of the thickness of the oxide shell. The dependencies in Figure 6 are of the same type showing the decreasing in the critical energy density from 15 nm to the minimal point and then increasing. The minimum position is a function of the oxide shell thickness; the thickness increasing leads to the optimal radius of the nanoparticle rising.

This trend could be also found from the equation (5). The minimum positions (minimal H_c and respective R values) at several shell thickness values are presented in Table. The optimal radius of the metal nanoparticle existing in terms of the model could be determined in two ways: (i) one is able to find the radius of the most heated nanoparticle in the under-threshold mode; (ii) one can calculate the dependence of critical energy density on the nanoparticle's radius and find its minimum. The existence of the optimal radius of the nanoparticle providing the minimal energy density other conditions are the same is inherited in the model taking into account the oxide shell from the initial model of the entirely metallic particles. As in the model a new parameter appears that is shell thickness, it is not surprising that optimal radius becomes its function. The optimal radius increases when the oxide shell becomes thicker, for instance, when the shell thickness increase from 0 to 10 nm the optimal radius increases in 1.5 times.

T a b l e

Minimum coordinates on the critical energy dependence on the nanopartciles radius at fixed oxide shell thickness values

L, нм	0	3	5	7	10
H_c, mJ/cm^2	58,7	67,3	71,2	75,1	80,8
R_m, nm	66,18	68,08	79,71	86,27	96

Conclusion

The model describing the laser initiation of explosive linked with radiative heating of metal nanoparticle with oxide shell in the explosive matrix was developed and analyzed. We showed that the optimal radius of the nanoparticle providing the minimum threshold of the ignition depends on the oxide shell thickness. The model is a new step towards application of the hot-spot theory to real explosive-metal nanopartilces composites. The optical properties will be incorporated in the future which will make it possible to compare the calculation results with the experimental one.

This research was funded by the Ministry of Science, Higher Education and Youth Policy of Kuzbass (agreement No. 5 dated Nov.11, 2022).

References

1 Aduev, B.P., Nurmukhametov, D.R., Furega, R.I., Zvekov, A.A., & Kalenskii, A.V. (2013). Explosive Decomposition of PETN with Nanoaluminum Additives under the Influence of Pulsed Laser Radiation at Different Wavelengths. *Russian Journal of Physical Chemistry B, 7*(4), 453–456. https://doi.org/10.1134/S199079311304012X

2 Aduev, B.P., Nurmukhametov, D.R., Zvekov, A.A., & Nelyubina, N.V. (2014). Influence of the mass fraction of oxide in aluminum nanoparticles on the explosive decomposition threshold and light absorption efficiency in petn-based compounds. *Combustion, Explosion, and Shock Waves,* 50(5), 578–581. https://doi.org/10.1134/S001050821405013X

3 Kalenskii, A.V., Anan'eva, M.V., Galkina, E.V., Kriger, V.G., & Zvekov, A.A. (2018). Micro hot-spot model of thermal explosion taking into account dielectric shell of sensitizing nanoparticle. *Journal of Physics: Conference Series*, 1115, 052017. https://doi.org/10.1088/1742-6596/1115/5/052017

4 Yang, J., Zhang, Gu-D., Zhang, J.-G., Chen, D., & Zhang, Qi. (2022). New perspectives on the laser initiation for metal tetrazine complexes: a theoretical study. *Phys Chem Chem Phys*, 24, 305–312. https://doi.org/10.1039/D1CP02319E

5 Lang, Q., Li. X., Zhou, J., Xu, Y., Lin, Q., & Lu, M. (2023). Two silver energetic coordination polymers based on a new N-amino-contained ligand: Towards good detonation performance and excellent laser-initiating ability. *Chemical Engineering Journal*, 452, 139473. https://doi.org/10.1016/j.cej.2022.139473

6 Akhmetshin, R., Razin, A., Ovchinnikov, V., Skripin, A., Tsipilev, V., Oleshko, V., Zarko, V., & Yakovlev, A. (2014). Effect of laser radiation wavelength on explosives initiation thresholds. *Journal of Physics: Conference Series*, 552, 012015. https://doi.org/10.1088/1742-6596/552/1/012015

7 Aduev, B.P., Nurmukhametov, D.R., Belokurov, G.M., Nelyubina, N.V., Kalenskii, A.V., & Aluker, N.L. (2017). Spectrokinetic characteristics of light emission at the early stages of the laser-initiated explosive decomposition of petn-based composites containing metal nanoparticle inclusions. *Russian Journal of Physical Chemistry B, 11*(3), 460–465. https://doi.org/10.1134/S1990793117030137

8 Kalenskii, A.V., Zvekov, A.A., Anan'eva, M.V., Nikitin, A.P., & Aduev, B.P. (2017). Effect of multiple scattering on the critical density of the energy used to initiate a PETN–aluminum compound by a neodymium laser pulse. *Combustion, Explosion, and Shock Waves, 53*(1), 82–92. https://doi.org/10.1134/S0010508217010129

9 Aduev, B.P., Nurmukhametov, D.R., Kolmykov, R.P., Nikitin, A.P., Anan'eva, M.V., Zvekov, A.A., & Kalenskii, A.V. (2016). Explosive decomposition of pentaerythritol tetranitrate pellets containing nickel nanoparticles with various radii. *Russian Journal of Physical Chemistry B, 10*(4), 621–627. https://doi.org/10.1134/S1990793116040187

10 Kalenskii, A.V., Anan'eva, M.V., Zvekov, A.A., & Zykov, I.Yu. (2015). Explosive decomposition kinetics of tetranitropentaerythrite aluminum pellets. *Technical Physics, 60*(3), 437–441. https://doi.org/10.1134/S1063784215030081

11 Fang, X., Stone, M., & Stennett, Ch. (2020). Pulsed laser irradiation of a nanoparticles sensitised RDX crystal. *Combustion and Flame*, 214, 387–393. https://doi.org/10.1016/j.combustflame.2020.01.009

12 Fang, X., Stennett, Ch., & Gaulter, S. (2023). Enhancement of laser ignitibility of insensitive energetic materials (FOX-7). *Propellants, Explos., Pyrotech*., 48, e202300079. https://doi.org/10.1002/prep.202300079

13 Fang X., & Walton, A.J. (2023). Optical sensitising of insensitive energetic material for laser ignition. *Optics & Laser Technology*, 158, 108767. https://doi.org/10.1016/j.optlastec.2022.108767

14 Bai, W., Wang, L., Tang, D., Yang, F., Qiao, Z., Lin, D., He, R., Zhu, W., & Qin, W. (2022). Constructing hotspots through star-shaped gold-copper alloy nanocrystals for laser initiation of explosives. *Optics & Laser Technology*, 152, 108120. https://doi.org/10.1016/j.optlastec.2022.108120

15 Bai, W., Qin, W., Tang, D., Ji, F., Chen, H., Yang, F., Qiao, Zh., Duan, T., Lin, D., He, R., Zhu, W., & Wang, L. (2021). Constructing interparticle hotspots through cracking silver nanoplates for laser initiation of explosives. *Optics & Laser Technology*, 139, 106989. https://doi.org/10.1016/j.optlastec.2021.106989

16 Alexandrov, E.I., & Tsipilev, V.P. (1984). Effect of the pulse length on the sensitivity of lead azide to laser radiation. *Combustion, Explosion and Shock Waves, 20*(6), 690–694. https://doi.org/10.1007/BF00757322

17 Zvekov, A.A., Nikitin, A.P., Galkina, E.V., & Kalenskii, A.V. (2016). The dependence of the critical energy density and hot-spot temperature on the radius metal nanoparticles in PETN. *Nanosystems: physics, chemistry, mathematics, 7*(6), https://doi.org/1017–1023. 10.17586/2220-8054-2016-7-6-1017-1023

18 Kalenskii, A.V., Zvekov, A.A., Nikitin, A.P., Anan'eva, M.V., & Aduev, B.P. (2015). Specific Features of Plasmon Resonance in Nanoparticles of Different Metals. *Optics and Spectroscopy, 118*(6), 978–987. https://doi.org/10.1134/S0030400X15060119

19 Zvekov, A.A., Aduev, B.P., Anan'eva, M.V., Kalenskii, A.V., & Galkina, E.V. (2019). Method for calculating the optical properties of composites based on a transparent matrix with residual porosity and metal nanoparticles. *Journal of Applied Spectroscopy, 86*(3), 470–478. https://doi.org/10.1007/s10812-019-00843-z

20 Kalenskii, A.V., Gazenaur, N.V., Zvekov, A.A., & Nikitin, A.P. (2017). Critical conditions of reaction initiation in the petn during laser heating of light-absorbing nanoparticles. *Combustion, Explosion, and Shock Waves, 53*(2), 219–228. https://doi.org/10.1134/S0010508217020137

А.А. Звеков, А.В. Каленский, А.П. Боровикова, Е.В. Галкина, П.О. Винодиктов

Оксидті қабықшаның жарылғыш ыдырауы бар металл нанобөлшектерімен легирленген энергетикалық материалдардың лазерлік инициациясы

Мақала лазерлік инициациялық композициялық материалдардың оксидті қабықпен қапталған металл нанобөлшектері бар жарылғыш матрица болуын сипаттайтын модельді әзірлеуге арналған. Модельде оксид қабығын жарықты сіңірмейтін диэлектрик ретінде қарастырады. Негізгі нәтижелер алюминий оксидімен қапталған алюминий нанобөлшектеріне арналған. Модель шеңберінде «металл ядросы–оксидті қабық–жарылғыш зат» жүйесіндегі жылу беру процестері, Аррениус температурасына тәуелділікпен бірінші ретті реакция ретінде модельденген жарылғыш заттың экзотермиялық ыдырауы және «ядро–қабық» шекарасындағы сәулелендуді сіңіру зерттелген. Модель дифференциалдық теңдеулер жүйесі түрінде жазылып, сандық орындауға арналған компьютерлік бағдарлама жасалған. Модельдің жартылай сандық талдауы сәулелену импульсінің әрекеті кезінде қыздырылған матрицалық қабаттың сипаттамалық қалыңдығын пайдалана отырып жүргізілді. Ең жоғары температураға жеткен нанобөлшектің радиусы қыздырылған матрицалық қабаттың қалыңдығына пропорционал болатыны көрсетілген, бұл модельдің алдыңғы нұсқасына сәйкес келеді, бірақ пропорционалдық коэффициенті оксид қабықшасының қалыңдығына байланысты. Модельге сандық талдау жасалды. Инициация энергиясының критикалық тығыздығының нанобөлшектің тұрақты радиусындағы оксид қабығының қалыңдығына және қабықтың тұрақты қалыңдығындағы нанобөлшек радиусына тәуелділігі есептеледі. Радиусқа тәуелділік минималды инициация шегіне әкелетін оңтайлы нанобөлшектің болуын көрсетеді. Оңтайлы нанобөлшектің радиусы қабықтың қалыңдығына байланысты.

Кілт сөздер: лазерлік инициация, термиялық жарылыс, ыстық нүкте моделі, ядро қабықшасының нанобөлшектері, энергетикалық материалдар.

А.А. Звеков, А.В. Каленский, А.П. Боровикова, Е.В. Галкина, П.О. Винодиктов

Закономерности лазерного инициирования взрыва энергетических материалов, допированных наночастицами

Статья посвящена развитию модели лазерного инициирования взрыва композитных материалов, представляющих собой матрицу взрывчатого вещества, содержащую наночастицы металлов с оксидной оболочкой. В рамках модели оксидная оболочка рассмотрена как диэлектрик прозрачный для лазерного излучения. Основные результаты представлены для наночастиц алюминия, покрытых оксидом алюминия. В рамках модели изучены процессы теплопереноса в системе «металлическое ядро–оксидная оболочка–взрывчатое вещество», экзотермическое разложение взрывчатого вещества, моделируемое как реакция первого порядка с Аррениусовской температурной зависимостью, и поглощение излучения на границе «ядро–оболочка». Модель записана в виде системы дифференциальных уравнений, и разработана компьютерная программа для численной реализации. Выполнен полуколичественный анализ модели с использованием величины характерной толщины слоя прогретой матрицы за время действия импульса излучения. Показано, что радиус наночастицы, достигающей наибольшей температуры, пропорционален толщине прогретого слоя матрицы, что согласуется с предыдущим вариантом модели, однако коэффициент пропорциональности зависит от толщины оксидной оболочки. Проведен численный анализ модели. Рассчитаны зависимости критической плотности энергии инициирования от толщины оксидной оболочки при постоянном радиусе наночастицы и радиуса наночастицы при постоянной толщине оболочки. Зависимость от радиуса свидетельствует о существовании оптимальной наночастицы, приводящей к минимальному порогу инициирования. Радиус оптимальной наночастицы зависит от толщины оболочки.

Ключевые слова: лазерное инициирование, тепловой взрыв, микроочаговая модель, наночастицы, ядро–оболочка, энергетические материалы.

Information about the authors

Alexander Kalenskii (corresponding author) — Doctor of physical and math science, Head of the Department of Solid State Chemistry and Material Science, Kemerovo State University, Krasnaya st., 6, 650000, Kemerovo, Russia; *e-mail: kalenskyav@gmail.com*; https://orcid.org/0000-0002-6658-0787

Alexander Zvekov — Doctor of physical and math science, Professor, Department of Solid State Chemistry and Material Science, Kemerovo State University, Krasnaya st., 6, 650000, Kemerovo, Russia; *e-mail: zvekovaa@gmail.com*, https://orcid.org/0000-0002-2941-9783

Anastasia Borovikova — Candidate of physical and math science, Head of Scientific and Innovation Office, Kemerovo State University, Krasnaya st., 6, 650000, Kemerovo, Russia; *e-mail: science@kemsu.ru*, https://orcid.org/0000-0002-4987-3406

Elena Galkina — Candidate of physical and math science, Tutor, Department of Solid State Chemistry and Material Science, Kemerovo State University, Krasnaya st., 6, 650000, Kemerovo, Russia; *e-mail: keltrilla@gmail.com*

Pavel Vinodiktov — 2nd year PhD student, Kemerovo State University, Krasnaya st., 6, 650000, Kemerovo, Russia; *e-mail: vinodiktovpavel@yandex.ru*